HYPERON-NUCLEON INTERACTION, HYPERNUCLEI AND HYPERONIC MATTER

ISAAC VIDAÑA

Centro de Física Computacional. Department of Physics. University of Coimbra, PT-3004-516 Coimbra, Portugal

ABSTRACT

Strangeness adds a new dimension to the evolving picture of nuclear physics giving us an opportunity to study the fundamental baryon-baryon interactions from an enlarge perspective. The presence of hyperons in finite and infinite nuclear systems constitute a unique probe of the deep nuclear interior which makes possible to study a variety of otherwise inaccessible nuclear phenomena, and thereby to test nuclear models. Furthermore, there is a growing evidence that strange particles can have significant implications for astrophysics. In particular, the presence of hyperons in the dense inner core of neutron stars is expected to have have important consequences for the equation of state, struture and evolution of such compact objects. In this lecture we will disuss several topics of hypernuclear physics. After a introduction and historical overview, we will address different aspects of the production, spectroscopy and decay of hypernuclei. Then we will present several models for the hyperon-nucleon interaction, and finally, we will examine the role of hyperons on the neutron star properties.

I – INTRODUCTION AND HISTORICAL OVERVIEW

Hypernuclei are bound systems composed of neutrons, protons and one or more hyperons (i.e., baryons with strange content). They were first observed in 1952 with the discovery of a hyperfragment by Danysz and Pniewsli in a balloon-flown emulsion stack [1]. The initial cosmic-ray observations of hypernuclei were followed by pion and proton beam production in emulsions and then in ^{4}He bubble chambers. The weak decay of the Λ particle into a π^- plus a proton was used to identify the Λ-hypernuclei and to determine binding energies, spins and lifetimes for masses up to A=15 [2,3]. Average properties of heavier systems were estimated from spallation experiments, and two double-Λ hypernuclei were reported from Ξ^- capture [4,5]. More systematic investigations of hypernuclei began with the advent of separated K^- beams, which permitted the realization of counter experiments [6].

Although major achievements in hypernuclear physics have been taken very slowly due to the limited statistics, the in-flight (K^-,π^-) counter experiments carried out at CERN [7,8] and Brookhaven (BNL) [9] have revealed a considerable amount of hypernuclear features such as that the Λ particle essentially retains its identity in a nucleus, the small spin-orbit strength, or the nowadays discarded, narrow widths of Σ-hypernuclei, injecting a renewed interest in the field. Since then, the experimental facilities have been upgraded and experiments using the (π^+,K^+) and ($K^-_{stopped},\pi^0$) reactions are being conducted at the Brookhaven AGS and KEK accelerators with higher intensities and improved energy resolution of the beams.

The electromagnetic production of hypernuclei at the Thomas Jefferson National Laboratory (JLAB), through the reaction (e,e'K^+), promises to provide a new high-precision tool to study Λ-hypernuclear spectroscopy, with resolutions of several hundred keV [10]. In addition, the study of electromagnetic decay of hypernuclear levels using large-solid angle germanium (Ge) dectectors, should help to define the spectra of lighter hypernuclei. It is also possible that more intense beams of kaons and heavy ions, coupled with new detection technologies, may provide the means to detect multi-strange hypernuclei [11].

In connection with this latter aspect, much less is known about Ξ-hypernuclei or double Λ hypernuclei [12]. From the point of view of the conventional many-body problem, a study of the hyperon-hyperon interaction is very important, and it can be done within a multi-strange hypernucleus. Of course a direct study of the hyperon-hyperon scattering would be extremely valuable, but because these paricles have very short lifetimes, this is not possible. Still, there are emulsion events which have been interpreted as either Ξ- or double-Λ hypernuclei. These events, if interpreted correctly, would give the well depth for the $\Lambda\Lambda$ potential [13].

From the theoretical side, one of the goals of hypernuclear research is to relate hypernuclear observables to the bare hyperon-nucleon (YN) and hyperon-hyperon (YY) interactions. The experimental difficulties associated with the short lifetime of hyperons and low intensity beam fluxes have limited the number of ΛN and ΣN scattering events to less than one thousand [14-18], not being enough to fully constraint the YN interaction. In the absence of such data, alternative information on the YN and YY interactions can be obtained from the study of hypernuclei. One possibility is to focus on light hypernuclei, such as $^3H_\Lambda$,$^3He_\Lambda$ and $^4He_\Lambda$, which can be treated "exactly" by solving the 3-body Faddeev [19,20] and 4-body Yakubovky [21] equations. However, the power of these techniques is limited by the scarce amount of spectroscopic data. Only the ground states energies and a particle stable excited states for each A=4 species can be used to put further constraints on the interaction. Another possibility is the study of hypernuclei with larger masses.

Attempts to derive the hyperon properties in a finite nucleus have followed several approaches. Traditionally, they have been reasonably well described by a shell-model picture using Λ-nucleus potentials of the Woods-Saxon type that reproduce quite well the measured hypernuclear states of medium to heavy hypernuclei [22-24]. Non-localities and density dependent effects, included in non-relativistic Hatree-Fock calculations using Skyrme YN interactions [25-29] improve the overall fit to the single-particle binding energies. The properties of hypernuclei have also been studied in a relativistic framework, such as Dirac phenomenology, where the hyperon-nucleus potential has been derived from the nucleon-nucleus one [30,31], or relativistic mean field theory [32-39].

Microscopic hypernuclear structure calculations, which provide the desidered link of the hypernuclear observables to the bare YN interaction, are also available. They are based on the construction of an effective YN interaction (G-matrix) which is obtained from the bare YN potential through a Bethe-Goldstone equation. In earlier microscopic calculations, Gaussian parametrizations of the G-matrix calculated in nuclear matter at an average density were employed [40-43]. A G-matrix obtained directly in finite nuclei was used to study the single-particle energy levels in various hypernuclei [44]. Nuclear matter G-matrix elements were also used as an effective interaction in a calculation of the $^{17}O_\Lambda$ spectrum [45]. The s- and p-wave Λ single-particle properties for a variety of Λ-hypernuclei, from $^5He_\Lambda$ to $^{208}Pb_\Lambda$, where derived in Refs. [46-47] by constructing a finite nucleus YN G-matrix from a nuclear matter G-matrix.

In addition to hypernuclei, nuclear physicist have also been interested in hyperonic matter (nuclear matter with nucleonic and hyperonic degrees of freedom), especially in connection with the physics of neutron star interiors. These objects are an excellent observatory to test our understanding of the theory of strong interacting matter at extreme densities. The interior of

neutron stars is dense enough to allow for the appearance of new particles with strangeness content besides the conventional nucleons and leptons by virtue of the weak equilibrium. There is a growing evidence that hyperons appear as the first strange baryons in neutron star matter at around twice normal nuclear saturation density [48], as has been recently confirmed with effective non-relativistic potential models [49], the Quark-Meson Coupling Model [50], extended relativistic mean field approaches [51,52], relativistic Hartree-Fock [53] and Brueckner-Hartree-Fock theory [54,55].

Properties of neutron stars are closely related to the underlying Equation of State (EoS) of matter at high densities. These properties are affected by the presence of strangeness [56,57]. A strong deloptenization of neutron star matter occurs when hyperons appear, since it is energetically more convenient to maintain charge neutrality through hyperon formation than from β-decay. In addition, it is clear that the main effect of the presence of hyperons in dense matter is to soften the EoS, which translates into a lower maximum mass of the neutron star [55]. Other properties, such as thermal and structural evolution of neutron stars, are also very sensitive to the composition and, therefore, to the strangeness content of neutron star interiors. From the observational point of view, measurements of the surface temperature of neutron stars, with satellite-base X-ray observatories, could tell us whether these exotic components of nuclear matter are playing a role in cooling processes. Furthermore, one of the major goals of the Laser Interferometer Gravitational-wave Observatory (LIGO) is to measure gravitational waves emitted in the coalescence of two neutron stars. The pattern of the emitted waves just prior to the merging is sensitive to the structure of the stars and to the EoS.

Although hyperonic matter is an idealized physical system, the theoretical determination of the corresponding EoS is an essential step towards the undertanding properties of neutron stars. In addition, the comparison of theoretical predictions for the properties of these objects with the observations can provide strong constraints on the interactions among their constituents. Therefore, a detailed knowledge of the EoS over a wide range of densities is required [58]. This is a very hard task from the theoretical point of view. Traditionally, two approaches have been followed to describe the baryon-baryon interaction in the nuclear medium and to construct from it the EoS of dense hadronic matter: the so-called phenomenological approach and the microscopic approach.

In the phenomenological approach the input is a density-denpendent effective interaction which contains a certain number of parameters adjusted to reproduce experimental data, such as the properties of nuclei, or the empirical saturation properties of nuclear matter. There exists an enormous number of different phenomenological interactions such as the Migdal [59] and Gogny [60] forces. But the most popular of them is the Skyrme interaction [61-62]. This force has gained so much importance because it reproduces the nuclear binding energies and the nuclear radii over the whole periodic table with a reasonable set of parameters [62]. There is a connection [63] between this force and the more fundamental G-matrix. Balberg and Gal [49,64] have recently derived an analytic effective EoS using density-dependent baryon-baryon potentials based on Skyrme-type forces including hyperonic degrees of freedom. The features of this EoS rely on the properties of nuclei for the nucleon-nucleon (NN) interaction, and mainly on the experimental data from hypernuclei for the YN and YY interactions. It reproduces typical properties of high-density matter found in theoretical microscopic models.

An alternative phenomenological approach involves the formulation of an effective relativistic mean field (RMF) theory of interacting hadrons [65-66]. This approach treats the baryonic and mesonic degrees of freedom explicitely, is fully relativistic, and is, in general, easier to handle because it only involves local densities and fields. The EoS of dense matter with hyperons was first described within the RMF by Glendenning [48,67,68]. The parameters of this approach are fixed by the properties of nuclei and nuclear bulk matter for the nucleonic sector, whereas the coupling constants of the hyperons are fixed by symmetry relations and hypernuclear observables.

In a microscopic approach, on the other hand, the input are two-body baryon-baryon interactions that describes the scattering observables in free space. These realistic interactions have been mainly constructed within the framework of a meson-exchange theory, although recently a new approach based on chiral perturbation theory has emerged as a powerful tool. In order to obtain the EoS one has to solve the complicated many-body problem. The main great difficulty of this problem lies in the treatment of the strong repulsive core, which dominates the short-range behaviour of the interaction. Various methods have been considered to solve the many-body problem, the most employed ones being the variational approach and the Brueckner-Bethe-Goldstone theory. Nevertheless, although both methods have been extensively applied to the study of nuclear matter, only the Brueckner-Bethe-Goldstone theory has been extended to the hyperonic sector [54,55].

To conclude we would like to stress that although hypernuclear physics is almost 60 years old, it is still a very active field of research. New experimental facilities under construction at GSI, JLAB, J-PARC and other sites will soon allow a much more precise determination of the properties of hyperon-nucleon and hyperon-hyperon forces than is currently available.

II – PRODUCTION, SPECTROSCOPY AND WEAK DECAY OF HYPERNUCLEI

In the following we will describe different production mechanis of hypernuclei. After that we will discuss some aspects of hypernuclear γ-ray spectroscopy. Finally, we will briefly present the different weak decay modes of hypernuclei.

IIa-. Production mechanisms of hypernuclei

Single-Λ hypernuclei can be produced by several mechanism such as:

Strangeness exchange reactions:

$$K^- + {}^A Z \rightarrow {}^A_\Lambda Z + \pi^-, \tag{1}$$

where a neutron hit by a K^- is changed into a Λ hyperon emiting a π^-. These experiments measure mainly the hyperon binding energies and allow the identification of excited hypernuclear levels. The hypernuclear mass, from which the hyperon binding energy can be deduced as

$$B_{{}^A_\Lambda Z} = B_{{}^A Z} + M_{{}^A Z} + M_\Lambda - M_N - M_{{}^A_\Lambda Z}, \tag{2}$$

is obtained by measuring both the incident K^- momentum and the out-going π^- momentum as follows

$$M_{{}^A_\Lambda Z} = \sqrt{\left(E_{\pi^-} - E_{K^-} - M_{{}^A Z}\right)^2 + \left(\vec{p}_{\pi^-} - \vec{p}_{K^-}\right)^2}. \tag{3}$$

Therefore, two magnetic spectrometer systems both with good energy resolution are required in order to achieve a good hypernuclear mass resolution.

In some cases a K^- beam, with rather low-momenta, is injected on thick nuclear targets that stop the K^- before it decays. The K^- looses its energy in the target, and is eventually trapped in atomic orbits of a kaonic atom through various atomic processes. The K^- is absorbed in the final stage by the atomic nucleus. The kaon capture process proceeds mainly with the emission of a pion an the formation of a the hypernucleus

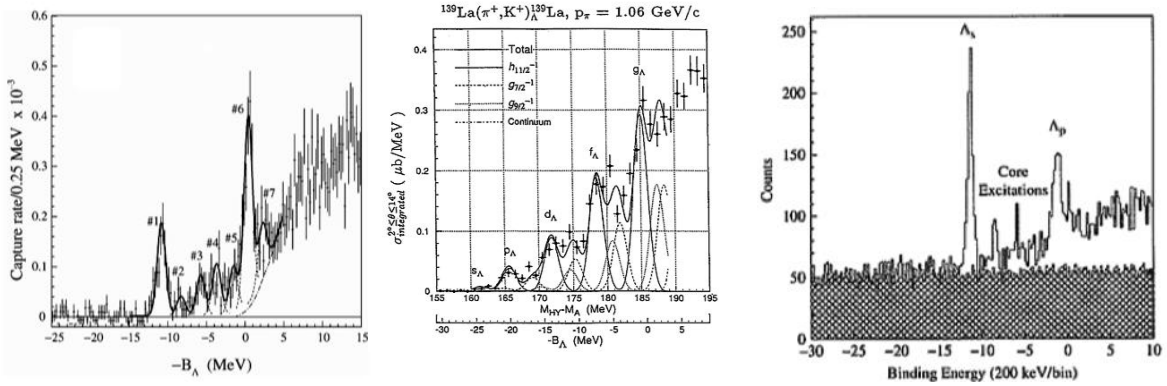

Figure 1. Hypernuclear spectrum of the $^{12}C_\Lambda$, $^{132}La_\Lambda$ and $^{12}B_\Lambda$ hypernuclei obtained respectively in a ($K^-_{stopped}$,π^-) experiment (left panel), a (π^+,K^+) reaction (middle panel) and by electro-production (right panel). Figures are adapted from Refs. [69], [70] and [71], respectively.

$$K^-_{stopped} + {}^A Z \rightarrow {}^A_\Lambda Z + \pi^- .$$

(4)

Since the reaction occurs essentially at rest, in this case it is necessary be to measure only the momemtum of the emitted pion in order to determine the hypernuclear mass

$$M_{{}^A_\Lambda Z} = \sqrt{\left(E_{\pi^-} - M_{K^-} - M_{{}^A Z}\right)^2 + p^2_{\pi^-}} . \quad (5)$$

Therefore, one magnetic spectrometer for π^- or a π^0 spectrometer detecting two gamma-rays from π^0 decay with good energy resolution is enough. The left panel of Fig. 1 shows as example the energy spectrum of the $^{12}C_\Lambda$ hypernucleus obtained in a ($K^-_{stopped}$,π^-) experiment.

Associate production reactions:

$$\pi^+ + {}^A Z \rightarrow {}^A_\Lambda Z + K^+ . \quad (6)$$

Here, an $s\bar{s}$ pair is created from the vacuum and a K^+ and a Λ are produced in the final state (the so-called associate production). The production cross section is reduced, compared to the strangeness exchange reaction, however this drawback is compensated by the greater intensities of the π^+ beams. The hypernuclear mass is obtained by measuring the π^+ momentum and the K^+ with two spectrometers as in the case of the (K^-,π^-) reaction. The middle panel of Fig. 1 shows as example the energy spectrum of the $^{139}La_\Lambda$ hypernucleus.

Electro-production reactions:

$$e^- + {}^A Z \rightarrow e' + K^+ + {}^A_\Lambda (Z-1). \quad (7)$$

This process is relatively new and promises to provide a new high-precision tool to study Λ-hypernuclear spectroscopy, with energy resolutions of several hundred keV [10]. At the present moment only two laboratories in the world, the JLAB (USA) and MAMI-C (Germany), have the instrumental capabilities to perform experiments on hypernuclear spectroscopy by using electron beams. The electron beams have excellent spatial and energy resolutions, so this reaction is used for studies of hypernuclear structure. A schematic layout of the experimental setup together with the experimental geometry is shown in Fig. 2.

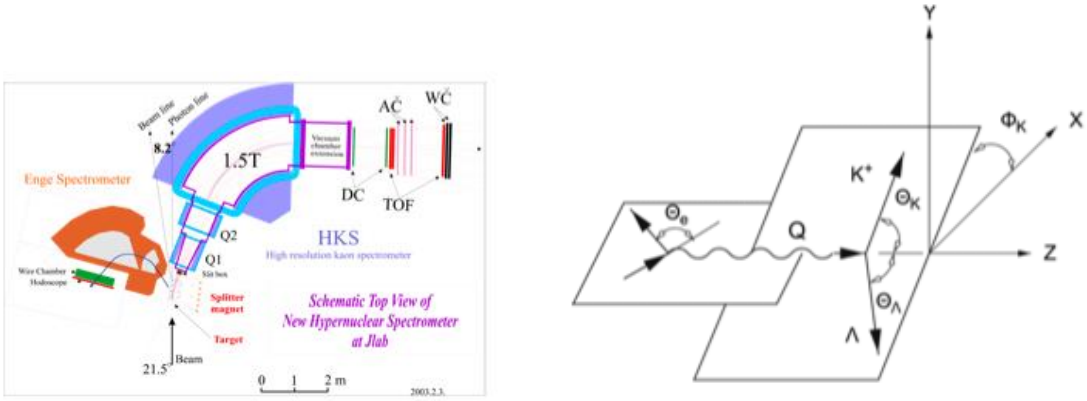

Figure 2. Schematic layout of the experimental set up and experimental geometry of the (e,e'K^+) reaction. Figures adapted from Ref. [72].

The electro-production of hypernuclei can be well described by a first order perturbation calculation as the exchange of a virtual photon between the electron and a proton of the nucleus, which is changed into a Λ hyperon (see Fig. 2). Although the cross section for kaon electro-production is about 2 orders of magnitude smaller than the (π^+,K^+) reaction, this can be compensated by larger electron beam intensities.

Since the cross section falls rapidly with increasing transfer momentum Q (see Fig. 2) and the virtual photon flux is maximized for an electron scatterig angle near zero degrees, experiments must be done within a small angular range around the direction of the virtual photon. The experimental geometry requires two spectrometers, one to detect the scattered electrons which defines the virtual photons, and one to detect the kaons. Both of these spectrometers must be placed at extremely forward angles. Because of this, a magnet is needed to deflect the electrons and kaons away from zero degrees into their respective spectrometers. In addition, since many pions, positrons and protons are transmitted through the kaon spectrometer, it is required an excellent particle identification not only in the hardware trigget, but also in the data analysis. By measuring the type of out-going particles and their energies ($E_{e'}$, E_K^+), and knowing the energy of the in-coming electron (E_e) it is possible to calculate the energy which is left inside the nucleus in each event:

$$E_x = E_e - E_{e'} - E_{K^+}, \tag{8}$$

from which it can be deduced the energy of the produced hypernuclei.

An example of the binding energy spectrum for the $^{12}B_\Lambda$ hypernucleus is shown in the right panel of Fig. 1. The two prominent peaks represent the nuclei in the ground state with the Λ particle in the s- and p-shell, respectively. The other peaks between them are the core excitations with nucleons in p-shell [73].

The kinematics for these elementary processes is shown in Fig. 3. As it can be seen in the figure, the n(K^-,π^-)Λ and n(K^-,π^-)Σ reactions can have low, essentially zero, momentum transfer to a produced Λ or Σ hyperon. Thus the probability that this hyperon will interact with, or be bound to, the spectator nucleons is large. On the other hand reactions such as n(π^+,K^+)Λ or p(γ,K^+)Λ have high momentum transfer with respect to the Fermi momentum, and produced recoil hyperons have a high probability of escaping the nucleus. The cross sections to bound states are reduced, when the momentum transfer is high.

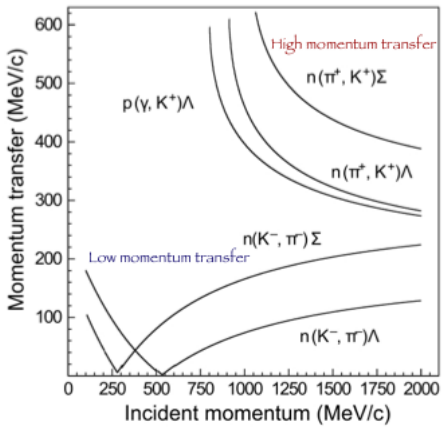

Figure 3. The recoil momentum of a hyperon in various elementary reactions at 0º as a function of the inciden particle momentum. Figure adapted from Ref. [72].

It is known that a K^- strongly interacts with nucleons through various resonant states (e.g., $\Lambda(1405)$). Therefore, incident kaons in a (K^-,π^-) reaction attenuate rapidly in nuclear matter, the K^- mostly interacts with an outer shell neutron with little momentum transfer, simply replacing it with a Λ in the same shell. On the other hand, energetic π^+ and K^+ have longer mean free paths in nuclear matter, and give longer momentum transfer to the hyperon. Thus they can interact with interior nucleons, and there can be significant angular momentum transfer.

Σ-hypernuclei are produced by the same mechanisms described above. Double-Λ hypenuclei cannot be produced in a single step process. To produce them, first it is necessary to create a Ξ^- through the reaction

$$K^- + p \rightarrow \Xi^- + K^+,$$
(9)

or

$$p + \bar{p} \rightarrow \Xi^- + \bar{\Xi}^+.$$
(10)

The Ξ^- should be then captured in an atomic orbital and interact with the nuclear core producing two Λ´s particles for example by

$$\Xi^- + p \rightarrow \Lambda + \Lambda + 28.5\,MeV.$$
(11)

This reaction provides about 30 MeV of energy that is equally shared between the two Λ´s in most cases, leading to the escape of one or both from the nucleus.

IIb-. Hypernuclear γ-ray spectroscopy

Hypernuclei can be produced in excited states if a nucleon in a p- or higher shell is replaced by a hyperon. The energy of this exicted states can be released either by emitting nucleons, or, sometimes, when the hyperon moves to lower energy states, by the emission of γ-rays. Measurements of γ-ray transitions in Λ-hypernuclei allow to analyze excited levels with an excellent energy resolution.

Nevertheless, there have been some technical difficulties to apply γ-ray spectroscopy to hypernuclear spectroscopy, mainly related with the detection efficiency of γ-ray measurements and

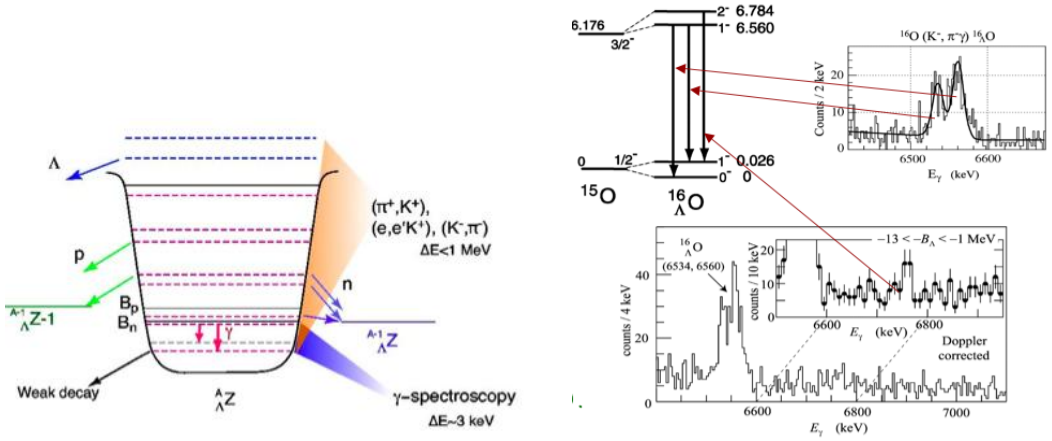

Figure 4. *Left:* Various decay schemes of Λ-hypernuclei. *Right:* γ transitions and the level schemes of $^{16}O_{\Lambda}$ measured recently at BNL. Figures adapted from Refs. [74] and [75].

with the necessity of covering a large solid angle with γ-ray detectors. These issues have been solved somehow with the construction of a large-acceptance germanium (Ge) detector array dedicated to hypernuclear γ-ray spectroscopy called *Hyperball*. There exist still, however, several weak points in hypernuclear γ-ray spectroscopy. A number of single-particle Λ orbits are bound in heavy Λ hypernuclei with a potential depth of around 30 MeV. However, the energy levels of many single-particle orbits are above the nucleon (neutron and proton) emission thresholds (see left side of Fig. 4). Thus, the observation of γ rays is limited to the low excitation region, maybe up to the Λ p orbit. Another weak point is the fact that γ-ray transition only measures the energy difference between two states. Therefore, single energy information is not enough to fully identify the two levels; the measurement of two γ-rays in coincidence might help to resolve it.

The right side of Fig. 4 shows as an exemple the γ transitions and the level schemes of $^{16}O_{\Lambda}$ identified and determined recently by γ-ray spectroscopy experiments at BNL. The γ-ray spectrum of $^{16}O_{\Lambda}$ have been measured using the (K^-,π^-) reaction. The observed twin peaks demonstrate the hypernuclear fine structure for $^{16}O_{\Lambda}$ $\left(1^- \rightarrow 1^-, 0^-\right)$ transitions. The small spacing in twin peaks is caused by the spin dependent ΛN interactions.

IIc-. Weak decay of Λ-hypernuclei

The main decay mode of a Λ particle in free space is the so-called mesonic weak decay mode

$$\Lambda \rightarrow N + \pi, \qquad p_N \sim 100\, MeV \tag{12}$$

where a Λ particle decays 64% of the times into a proton and a π^-, and 36% into a neutron and a π^0. This mode is strongly suppressed by the Pauli principle when the hyperon is bound in the nucleus, because the momentum of the out-going nucleon (around 100 MeV/c) is smaller than the typical Fermi momentum in nuclei (~270 MeV/c). The so-called non-mesonic decay mode, according to which the Λ interacts with one (or more) of the surrounding nucleons

$$\begin{aligned} &\Lambda + N \rightarrow N + N, \qquad p_N \sim 420\, MeV \\ &\Lambda + N + N \rightarrow N + N + N, \qquad p_N \sim 340\, MeV \end{aligned} \tag{13}$$

becomes therefore the dominant decay mode in hypernuclei, specially in medium and heavy hypernuclei.

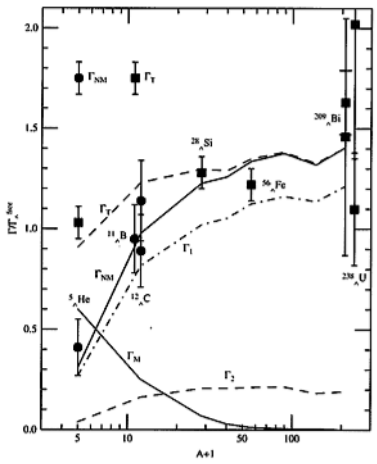

Figure 5. Weak decay rates as a function of the total number of particles. The figure has been adapted from Ref. [76].

Fig 5. shows the weak decay rates as a function of the total number of particles. The lines are theoretical estimations. The upper dashed line stands for the total decay rate, Γ_T, the decreasing solid line represents the mesonic decay mode Γ_M, while the increasing solid line represents the total non-mesonic decay rate Γ_{NM}, which corresponds to the sum of the one-nucleon (dot-dashed), Γ_1, and the two-nucleon induced mode (lower dashed line) Γ_2. Experimental values of the total and non-mesonic decay rates are given by the squares and circle marks respectively. As can be seen in the figure, the analysis of hypernuclear lifetimes as a function of the mass number, A, shows that the mesonic decay mode gets blocked as A increases, while the non-mesonic decay increases up to a saturation value of the order of the free Λ decay, reflecting the short-range nature of the weak ΔS=1 baryon-baryon interaction. The interested reader is referred to Refs. [76] and [77] and references therein for a detail discussion.

III – THE HYPERON-NUCLEON INTERACTION

Quantum chromodynamics (QCD) is commonly recognized as the fundamental theory of the strong interaction, and therefore, in principle, the baryon-baryon interaction can be completely determined by the underlying quark-gluon dynamics in QCD. Nevertheless, due to the mathematical problems raised by the non-perturbative character of QCD at low and intermediate energies (at this range of energies the coupling constants become too large for perturbative approaches), one is still far from a quantitative undertanding of the baryon-baryon interaction from the QCD point of view. This problem is, however, usually circumvented by introducing a simplified model in which only hadronic degrees of freedom are assumed to be relevant. Quarks are confined inside the hadrons by the strong interaction and the baryon-baryon force arises from meson exchange [78,79]. Such an effective description is presently the most quantitative representation of the fundamental theory in the energy regime of nuclear physics, although a big effort is being invested recently in understanding the baryon-baryon interaction from an Effective Field Theory perspective [80]. Quark degrees of freedom are expected to be important only at very short distances and high energies. Short-range parts of the interaction are treated, in all meson exchange model and effective field theory approaches, by including form factors which take into account, in an effective way, the extended structure of hadrons. In the next we briefly present the meson exchange and chiral effective field theory approaches of the hyperon-nucleon interaction.

The final part of this section will be devoted to the recent development of the low-momentum hyperon-nucleon interaction.

IIIa – Meson exchange model for the hyperon-nucleon interaction

The three relevant meson field types that mediate the interaction among the different baryons are: the scalar (s) field: σ,δ; the pseudoscalar (ps): π,K,η,η'; and the vector (v) fields: ρ,K^*,ω. Guided by symmetry principles, simplicity and physical intuition the most commonly employed interaction Lagrangians that couple these meson fields to the baryon ones are

$$L_s = g_s \overline{\Psi}\Psi\phi^{(s)} \tag{14}$$

$$L_{ps} = g_{ps} \overline{\Psi} i\gamma^5 \Psi\phi^{(ps)} \tag{15}$$

$$L_v = g_v \overline{\Psi}\gamma^\mu \Psi\phi_\mu^{(v)} + g_t \overline{\Psi}\sigma^{\mu\nu}\Psi\left(\partial_\mu\phi_\nu^{(v)} - \partial_\nu\phi_\mu^{(v)}\right) \tag{16}$$

for scalar, pseudoscalar and vector coupling, respectively. Alternatively, for the pseudoscalar field there is also the so-called pseudovector (pv) or gradient coupling, which is suggested as an effective coupling by chiral symmetry [81,82]

$$L_{pv} = g_{pv} \overline{\Psi}\gamma^5\gamma^\mu \Psi\partial_\mu\phi^{(ps)} \tag{17}$$

In the above expressions Ψ denotes the baryon fields for spin ½ baryons, $\phi^{(s)}$, $\phi^{(ps)}$ and $\phi^{(v)}$ are the corresponding scalar, pseudoscalar and vector fields, and the g's are the corresponding coupling constants that must be constrained by e.g. scattering data. Note that the above Lagrangians are for isoscalar mesons, however, for isovector mesons, the fields ϕ trivially modify to $\tau\cdot\phi$ with τ being the familiar isospin Pauli matrices.

Employing the above Lagrangians, it is possible to construct a one-boson-exchange (OBE) potential model. A typical contribution to the baryon-baryon scattering amplitude arising from the exchange of a certain meson ϕ is given by

$$\left\langle p'_1 p'_2 \left| V_\phi \right| p_1 p_2 \right\rangle = \frac{\overline{u}(p'_1) g_{\phi 1} \Gamma_\phi^{(1)} P_\phi u(p_1) \overline{u}(p'_2) g_{\phi 2} \Gamma_\phi^{(2)} P_\phi u(p_2)}{\left(p_1 - p'_1\right)^2 - m_\phi^2} \tag{18}$$

where m_ϕ is the mass of the exchanged meson, $P_\phi/((p_1-p_1')^2-m_\phi^2)$ represents the meson propagator, u and $\overline{u}$ are the familiar Dirac spinor and its adjoint ($\overline{u}u = 1, \overline{u} = u^+\gamma^0$), $g_{\phi 1}$, $g_{\phi 2}$ are the coupling constants at the vertices, and the Γ's denote the corresponding Dirac structures of the vertices

$$\Gamma_s^{(i)} = 1, \quad \Gamma_{ps}^{(i)} = i\gamma^5, \quad \Gamma_v^{(i)} = \gamma^\mu, \quad \Gamma_t^{(i)} = \sigma^{\mu\nu}, \quad \Gamma_{pv}^{(i)} = \gamma^5\left(\gamma^\mu \cdot \partial_\mu\right) \tag{19}$$

Expanding the free Dirac spinor in terms of 1/M (M is the mass of the relevant baryon) to lowest order leads to the familiar non-relativistic expressions for the baryon-baryon potentials, which through Fourier transformation give the configuration space version of the interaction. The general expression for the local approximation of the baryon-baryon interaction in configuration space is

$$V(r) = V_o(r) + V_s(r)(\vec{\sigma}_1 \cdot \vec{\sigma}_2) + V_t(r) S_{12} + V_{ls}(r)(\vec{L} \times \vec{S}^+) + V_{als}(r)(\vec{L} \times \vec{S}^-) \quad (20)$$

where V_0 is the central interaction, V_s the spin-spin part, V_t the familiar tensor term and V_{ls} and V_{als} the symmetric and antisymmetric spin-orbit pieces. Finally, one has to remember that in the meson exchange theory all meson-baryon vertices must be necessarily modified by the introduction of the so-called form factors. Each vertex is multiplied by a form factor of the type

$$F_\alpha(\vec{k}^2) = \left(\frac{\Lambda_\alpha^2 - m_\alpha^2}{\Lambda_\alpha^2 + \vec{k}^2} \right)^{n_\alpha} \quad (21)$$

or by

$$F_\alpha(\vec{k}^2) = e^{-\frac{\vec{k}^2}{2\Lambda_\alpha^2}}. \quad (22)$$

In Eq. (21) the quantity n_α is usually taken equal to 1 (monopole form factor) or 2 (dipole form factor). The vector $\vec{k}$ denotes the 3-momentum transfer, whereas Λ_α is the so-called cut-off mass, typically of the order 1.2 - 2 GeV. Originally the form factors were introduced for purely mathematical reasons, namely, to avoid divergences in the scattering equation. Nevertheless, our present knowledge of the (quark) substructure of baryons and mesons provides a physical reason for their presence. Obviously, it does not make sense to take the meson exchange picture seriously in a region in which modifications due to the extended structure of hadrons come into play.

Until now all that we have said is general and nothing has been commented yet about the specific hyperon-nucleon interaction. Presently there are in the market two different meson exchange models for the hyperon-nucleon interaction: the Jülich models [83,84] and the Nijmegen [85-88] ones. The main features of these two models are briefly presented in the following and the interested reader if referred to the original works for detailed information.

The Jülich hyperon-nucleon interaction is constructed in complete analogy to the Bonn nucleon-nucleon force [79]. It is defined in momentum space and contains the full energy-dependence and non-locality structure. Besides single-meson exchange processes, it includes higher-order processes involving π- and ρ-exchange processes (correlated 2π-exchange are conveniently parametrized in terms of an effective σ-exchange) and, in adition, KK, KK* and K*K* processes with N, Δ, Λ, Σ and Σ*(1385) intermediate states. Therefore, the model not only includes the couplings between the ΛN and ΣN channels, but also couplings to the $\Delta\Lambda$, $\Delta\Sigma$ and NΣ* ones. The exchange of pseudoscalar mesons η and η' is not considered. Parameters (coupling constants and cut-off masses) at NN and NΔ vertices are taken from the Bonn model. Coupling constants at the vertices involving strange particles are fixed by relating them, under the assumption of SU(6) symmetry, to the NN and NΔ values. Thus, the only free parameters are the cutt-off masses at the strange vertices which are adjusted to the existing hyperon-nucleon data. The form factors at the vertices are parametrized in the conventional monopole form or dipole form when the vertex involves both a spin-3/2 baryon and a vector meson.

The Nijmegen hyperon-nucleon interaction is obtained by a straightforward extension of the Nijmegen nucleon-nucleon model [89], through the application of SU(3) symmetry. It is defined both in momentum space and in configuration space. The model is generated by the exchange of nonets of pseudoscalar and vector mesons, and scalar mesons. Assuming SU(3) symmetry all the coupling constants at the vertices with strange particles are related to the NN ones. Gaussian form factors are taken at the vertices to guarantee a soft behaviour of the potentials in configuration space at small distances.

IIIb –Chiral Effective Field Theory for hyperon-nucleon interaction

Althought the meson-exchange picture provides a practical and systematic approach to the description of hadronic reactions in the low- and medium-energy regime, in the last decade chiral effective field theory (χEFT) has emerged as a new powerful tool. The derivation of the nuclear force from χEFT has been extensively discussed in the literature since the pioneering work of Weinberg [90]. The main advantage of this scheme is that there is an underlying power counting

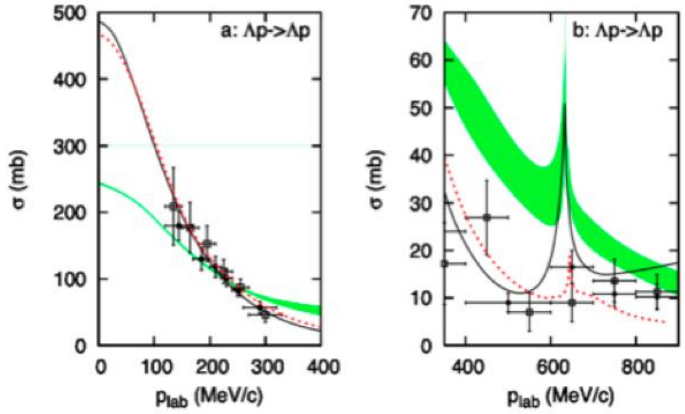

Figure 6. Λp total cross section as a function of the momentum in the lab frame. The figure has bee adapted from Ref. [96].

that allows to improve calculations systematically by going to higher orders in a perturbative expansion. In addition it is possible to derive two- and corresponding three-body forces as well as external current operators in a consistent way. The interested reader is referred to Refs. [91-93].

Recently the NN interaction has been described to high precision using χEFT [94,95]. In those works, the power counting is applied to the NN potential, which consists of pion exchanges and a series of contact interactions with an increasing number of derivatives to parametrize the shorter part of the NN force. A regularized Lipmann-Schwinger equation is solved to calculate observable quantities.

Contrary to the NN case, there are very few investigations of the YN interaction using χEFT. A recent application of the scheme used in Ref. [95] to the YN interaction has been performed by the Bonn-Jülich group [96]. A brief description of the procedure followed by the authors of Ref. [96] and of their results is shown in the following lines.

Analogous to the NN potential, at leading order (LO) in the power counting, the YN potential consist of pseudoscalar-meson exchanges and of four-baryon contact terms, where each of these two contributions is constrained via $SU(3)_f$ symmetry. The Lagrangian densities of the contact terms read

$$L^1 = C_i^1 \left\langle \overline{B}_a \overline{B}_b \left(\Gamma_i B\right)_b \left(\Gamma_i B\right)_a \right\rangle, \tag{23}$$

$$L^2 = C_i^2 \left\langle \overline{B}_a \left(\Gamma_i B\right)_a \overline{B}_b \left(\Gamma_i B\right)_b \right\rangle, \tag{24}$$

and

$$L^3 = C_i^3 \left\langle \overline{B}_a \left(\Gamma_i B\right)_a \right\rangle \left\langle \overline{B}_b \left(\Gamma_i B\right)_b \right\rangle .$$

(25)

Here, the labels a and b are the Dirac indices of the particles, Γ_i denotes the five elements of the Clifford algebra, Γ_1=1, $\Gamma_2=\gamma^\mu$,$\Gamma_3=\sigma^{\mu\nu}$, $\Gamma_4=\gamma^\mu\gamma^5$, $\Gamma_5=\gamma^5$ and B is the usual irreducible baryon octet representation of $SU(3)_f$. The Clifford algebra are here actually diagonal 3x3 matrices in the flavor space. The brackets denote taking the trace in flavor space. In LO the Lagrangians give rise to six independent low-energy coefficients (LEC's): C_S^1, C_T^1, C_S^2, C_T^2, C_S^3 and C_T^3, where S and T refer to the central and spin-spin parts of the potential respectively. The contribution of the one-pseudoscalar exchanges is constructed following the procedure described in the previous section. The YN potential contructed in this way is then inserted in the Lipmann-Schwinger equation which is regularized with a cut-off regulator function of the type

$$F(p,p') = e^{-\frac{(p^4+p'^4)}{\Lambda^4}}, \qquad (26)$$

in order to remove high-energy components of the baryon and pseudoscalar meson fields.

Fig. 6 shows the Λp total cross section as a function of the mometum in the lab frame. The shaded band represents the results of the χEFT for values of the cut-off parameter Λ ranging from 550 to 700 MeV. For comparison also the results for the Jülich'04 [84] and the Nijmegen NSC97f [87] meson-exchange models are shown. A good description of the low-energy Λp scattering data is obtained with both the χEFT approach and the meson-exchange model as can be seen in the figure. The Λp cross sections show a clear cusp at the Σ^+n threshold. This cusp is very pronounced for the χEFT model but also in the case of NSC97f one. This effect is hard to see in the experimental data, since it occurs over a very narrow energy range. Note that χEFT predicts Λp cross sections that are too large are higher energies. This is related to the problem that some LO phase shift are too large at higher energies. In a next to leading order (NLO) calculation this problem will eventually vanish.

The YN interaction based on χEFT yields also a correctly bound hypertriton and predicts reasonable Λ separation energies for ${}^4H_\Lambda$ (see Ref. [96] for details).

In conclusion, the results obtained by the Bonn-Jülich group strongly suggest that the χEFT scheme applied originally to the NN interaction, also works well for the YN one.

IIIc – Low-momentum hyperon-nucleon interaction

Following the same idea that in the nucleon-nucleon case made possible to calculate an "universal" effective low-momentum potential $V_{low\ k}$ by using Renormalization Group techniques, recently, Schaefer et al. [97] have generalized this method to the hyperon-nucleon sector.

The effective low-momentum potential $V_{low\ k}$ is obtained by integrating out the high-momentum components of a realistic YN interaction. This is achieved by introducing a cutoff Λ for the intermediate momenta in the Lipmann-Schwinger equation such that the physical low-energy quantities are cutoff independent. This results in a modified Lipmann-Schwinger equation with a cutoff-dependent effective potential $V_{low\ k}$

$$T\left(k',k;k^2\right) = V_{lowk}\left(k',k\right) + \frac{2}{\pi} P \int_0^\Lambda dq q^2 \frac{V_{lowk}\left(k',q\right) T\left(q,k;k^2\right)}{k^2 - q^2}. \qquad (27)$$

By demanding $dT(k',k;k^2)/d\Lambda=0$, an exact Renormalization Group flow equation for $V_{low\ k}$ can be obtained

$$\frac{dV_{lowk}(k',k)}{d\Lambda}=\frac{2}{\pi}\frac{V_{lowk}(k',\Lambda)T(\Lambda,k;\Lambda^2)}{1-k^2/\Lambda^2}.$$

(28)

Integrating this flow equation one can obtain a phase-shift, energy independent, soft (i.e., without hard core) and hermitian low-momentum potential $V_{low\ k}$. Unfortunatelly, as it has already been said, contrary to the NN case there exist only few YN scattering data and hence the YN interaction is not well constrained.

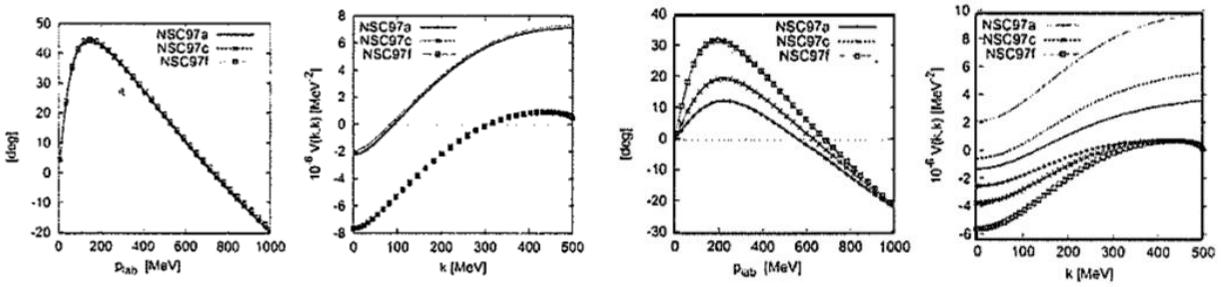

Figure 7. *Left panels:* $^1S_0$ phase shift and matrix elements for the isospin I=3/2 channel $\Sigma N \rightarrow \Sigma N$ *Right panels:* $^1S_0$ phase shift and matrix elements for the isospin I=1/2 channel $\Lambda N \rightarrow \Lambda N$. Results adapted from Ref. [97].

The left panels Fig. 7 show the $^1S_0$ phase shifts and matrix elements for the isospin I=3/2 channel $\Sigma N \rightarrow \Sigma N$ for several bare potentials and the corresponding $V_{low\ k}$ for a cutoff Λ=500 MeV as a function of the momentum in the lab frame. By construction the phase shifts are preserved. In the isospin I=1/2 channel the coupling $\Lambda N \rightarrow \Sigma N$, which has no counterpart in the NN case, has to be taken into account when generalizing the $V_{low\ k}$ approach to the YN case. The right panels of the figure show the corresponding results for the $\Lambda N \rightarrow \Lambda N$ $^1S_0$ partial wave where the $\Lambda N \rightarrow \Sigma N$ coupling has been taken into account. In this case, although, the phase shifts approximately obey the same shape they have different heights, and the diagonal matrix elements, although they collapse for momenta near the cutoff they differ for lower momenta. However, in conclusion, one can still say that in general the results seem to indicate a similar convergence to an "universal" softer low-momentum YN interaction as for the NN case.

IV- HYPERONIC MATTER AND NEUTRON STAR PROPERTIES

Neutron stars offer an interesting interplay between nuclear processes and astrophysical observables. Conditions of matter inside such objects are very different from those one can find on Earth, so a good knowledge of the Equation of State of dense matter is required to understand the properties of neutron stars. At densities near to the nuclear saturation density (ρ_0=0.16 fm^{-3}), matter is mainly composed of neutron, protons and leptons (electrons and muons) in β-equilibrium. As density increases, new hadronic degrees of freedom may appear in addition to neutrons and protons. One such degree of freedom is hyperons. Contrary to terrestial conditions, where hyperons are unstable and decay into nucleons through the weak interaction, the equilibrium conditions in neutron stars can make the inverse process happen, so the formation of hyperons becomes energetically favorable. In this section we will discuss the implications of hyperons on the Equation of State and structure of neutron stars.

IVa-. Basic properties and structure of neutron stars

A neutron star is the remnant of an ordinary star with a mass greater than ~ 5 $M_{\odot}$, where $M_{\odot}$ ~ 2 x 10^{33} g is the solar mass, after it has undergone a supernova explosion. A supernova explosion will occur when the star has exhausted its posibilities for energy production by nuclear fusion. The pressure gradient provided by radiation will then not be sufficient to balance the gravitational attraction, and the star becomes unstable. Eventually, it collapses. The inner dense regions of the star collapse first, and gravitational energy is released and transferred to the outer layers of the star, blowing them away. After the supernova explosion only a fraction of the star is left, and this final product might be a white dwarf, a neutron star or a black hole, depending on the inicial mass of the star.

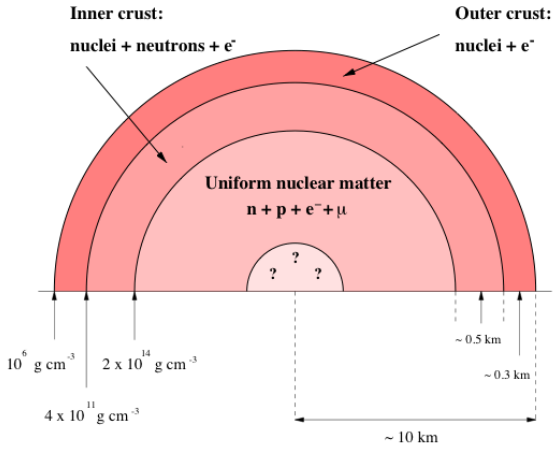

Figure 8. A schematic cross section of a neutron star illustrating the various regions discussed in the text.

Neutron stars are supported against gravitational collapse mainly by the neutron degeneracy pressure and may have typically masses of the order (1-2) $M_{\odot}$ and radii ~ 10 km. Such masses and radii yield an averaged density for neutron stars of order 10^{14}-10^{15} g/cm^3 . However, the expected densities in neutron stars span a rather wide range and in fact the internal structure of a neutron star can be described by an “onion” model. In Fig. 8 a schematic cross section of a neutron star is shown. The outer crust, with densities ranging from 10^6 g/cm^3 to 4 x 10^{11} g/cm^3, is a solid region where heavy nuclei, mainly around the iron mass number, in a Coulomb lattice coexist in β-equilibrium with an electron gas. When the density increases, the electron chemical potencial goes up and then, the electronic capture process

$$p + e^- \rightarrow n + \upsilon_{e^-},$$

(29)

opens, the nuclei becoming more and more neutron rich. The only available levels for neutrons at ~ 4.3 x 10^{11} g/cm^3 are in the continuum, and thus they start to “drip out” of the nuclei. We have then reached the inner crust, consisting of a Coulomb lattice of very neutron-rich nuclei together with a superfluid neutron gas and an electron gas with densities going from 4 x 10^{11} g/cm^3 to 2 x 10^{14} g/cm^3. At density ~ 10^{14} g/cm^3, nuclei start to dissolve and one enters the quantum fluid interior. In this region matter is mainly componed of superfluid neutrons with a smaller concentration of superconducting protons and normal electrons and muons [98]. In the core of the star, the density is of the order of 10^{15} g/cm^3. The composition of this region is not well known, and thus is subject to much speculation. Suggestions range from a mixed phase of quark and hadronic

matter [99,100], kaon or pion condensates [101-103], and hyperonic matter [54,55,99], which is the subject of this section.

A neutron star is one of the densest objects in the universe, therefore Einstein's General Relativity Theory is needed in order to determine its structure. Einstein's equations for a spherical static star take the form of the familiar Tolman-Oppenheimer-Volkoff (hereafter TOV) equations [104,105]

$$\frac{dp(r)}{dr} = -\frac{GM(r)\varepsilon(r)}{r^2}\left(1+\frac{p(r)}{\varepsilon(r)c^2}\right)\left(1+\frac{4\pi r^3 p(r)}{M(r)c^2}\right)\left(1-\frac{2GM(r)}{rc^2}\right)^{-1} \tag{30}$$

$$\frac{dM(r)}{dr} = 4\pi r^2 \varepsilon(r). \tag{31}$$

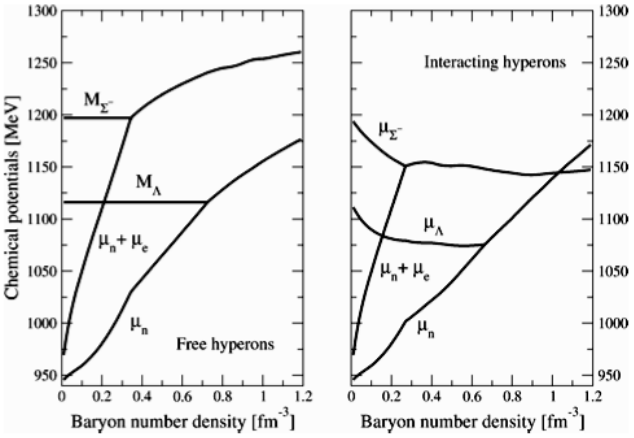

Figure 9. Chemical potentials in β-stable matter as a function of the total baryonic density. *Left panel:* free hyperons. *Right panel:* interacting hyperons.

The interpretation of the TOV equations is quite instructive. Think of a shell of matter in the star of radius r and thickness dr. Eq. (31) gives the mass-energy in this shell. The pressure of matter exterior to the shell is p(r) and interior to it p(r)+dp(r). The left side of Eq. (30) is the net force acting outward on the surface of the shell by the pressure difference dp(r) and the first factor on the right side is the attractive Newtonian force of gravity acting on the shell by the mass interior to it. The remaining factors are the exact corrections for General Relativity. So the TOV equations express the balance at each r between the internal pressure as it supports the overlying material against the gravitational attraction of the mass-energy interior to r. They are just the equations of hydrostatic equilibrium in General Relativity.

The Equation of State (EoS) p=p(ε) is the manner in which matter enters the equations of stellar structure. For a given EoS, the TOV equations can be integrated from the origin with the initial conditions that M(0)=0 (since near r=0 we may write $M(r)\sim 4\pi r^3\varepsilon(0)/3$), and an arbitrary value for the central energy density ε(0), until the pressure becomes zero. Zero pressure can support no overlying material against the gravitational attraction exerted on it from the mass within and so marks the edge of the star. The point R where the pressure vanishes defines the radius of the star and M(R) its gravitational mass,

$$M_G \equiv M(R) = 4\pi \int_o^R r^2 \varepsilon(r) dr \tag{32}$$

Neutron stars are, however, rotating objects. Rotation is expected to flatten the star more or less depending on its angular velocity. Spherical symmetry is thereby broken, although the star maintains its axial symmetry. This symmetry breaking makes the equations of structure much more
complicated. In addition to Eqs. (30) and (31) new complicated equations need to be solved. The interested reader is refered to Ref. [106] for explicit details of the equations.

Vb-. Neutron stars as "giant hypernuclei"

In a conservative and oversimplified picture the core of a neutron star is modeled as an uniform fluid of neutron rich nuclear matter in equilibrium with respect to weak interactions (β-stable nuclear matter). The presence of hyperons in neutron stars was first proposed in 1960 by Ambartsumyan and Saakyan [107], and since then it has been investigated by many authors. The reason why hyperons are expected in the high dense core of a neutron star is very simple, and its mainly a consequence of the fermionic nature of nucleons, which makes the nucleon chemical potential a

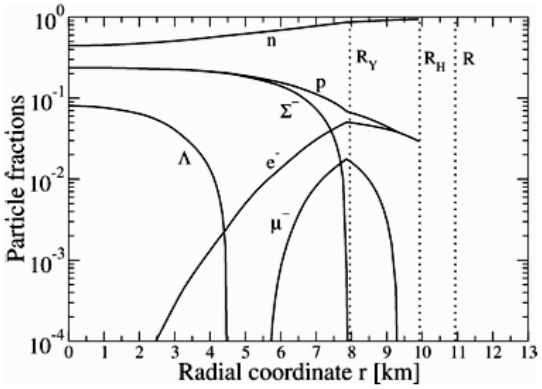

Figure 10. The internal composition of a neutron star with a hyperonic matter core. R_Y is the radius of the hyperonic core. The nuclear matter layer extends between R_Y and R_H and has about 2 km. The stellar crust extends between R_H and R and is about 1 km thick. The figure has been adapted from Ref. [108].

very rapidly increasing function of density. As soon as the chemical potential of neutrons becomes sufficiently large (see Fig. 9), the most energetic neutrons (i.e., those on the Fermi surface) can decay via the weak interactions into Λ hyperons and form a Fermi sea of this new hadronic species with $\mu_\Lambda=\mu_n$. The Σ^- can be produced via the weak process

$$e^- + n \rightarrow \Sigma^- + \nu_e, \tag{33}$$

when the Σ^- chemical potential fullfill the condition $\mu_\Sigma=\mu_n+\mu_e$ (Note that except from the very initial stage soon after neutron star birth, neutrinos freely escape the star and thus the neutrino chemical potential has not to be considered in the chemical equilibrium equations). As it can be seen from the results depicted in Fig. 9, hyperons appear at a relatively moderate density of about 2 times the normal saturation density of nuclear matter. Notice that the Σ^- hyperon appears at a lower density than the Λ, even though the Σ^- is more massive than the Λ. This is due to the contribution of the electron chemical potential μ_e to the threshold condition for the Σ^- (i.e., $M_\Sigma=\mu_n+\mu_e$ for free hyperons) and to the fact that μ_e in dense matter is large and can compensate for the mass difference $M_\Sigma - M_\Lambda = 81.76$ MeV.

In Fig. 10, it is shown the profile of such an hyperon star [108]. As it can be seen the hyperonic matter inner core of the star extends for about 8 km. This radius has to be compared with the total stellar core radius R ~ 11 km, and with the thickness of the nuclear matter layer (outer core) which is about 2 km. Thus one can conclude that neutron stars are “giant hypernuclei” [48] under the influence of gravity and strong interactions.

IVc-. Influence of hyperons on neutron star properties

The influence of hyperons on neutron star properties has been investigated using different approaches to determine the EoS of hyperonic matter. One of the most popular approaches, to solve this problem, is the relativistic mean field model [48]. Some of the parametrizations of the Lagrangian theory have tried to reconcile measured values of neutron star masses with the binding energy of the Λ particle in hypernuclei [109]. A different approach is based on the use of local effective potentials to describe the in-medium baryon-baryon interaction [49]. This method mimics

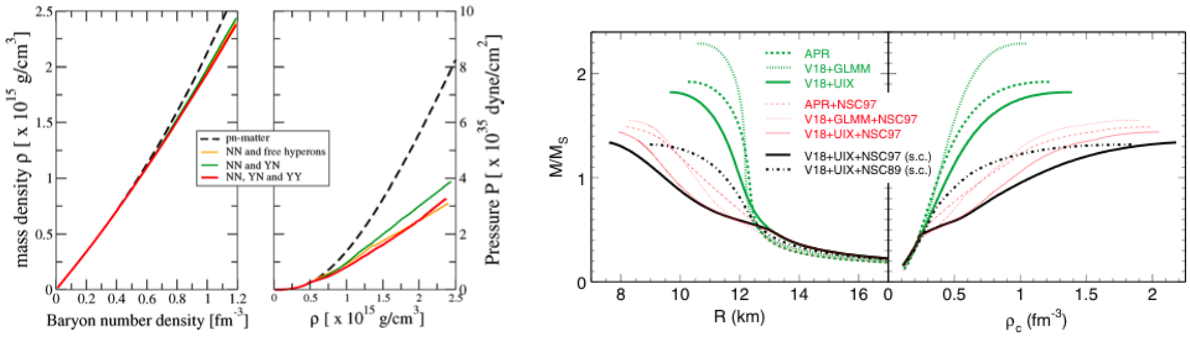

Figure 11. *Left panels:* Equation of State of hadronic matter with and without hyperons. *Right panels:* Mass-radius and mass-central density relations for different Equations of State with and without hyperons. See Refs. [55] and [110] for details.

and generalizes to the case of hyperonic matter the one based on the Skyrme nuclear interaction in the case of nuclear matter. A third approach, based on an extension of the Brueckner-Bethe-Goldstone (BBG) theory to include hyperonic degrees of freedom, starts from the basic baryon-baryon interaction and solve the many-body problem to get the EoS for hyperonic matter [54,55].

In the left panels of Fig. 11, it is shown the EoS for β-stable matter obtained obtained the Brueckner-Hartree-Fock (BHF) approximation of the extended BBG theory [55]. As expected, the presence of hyperons makes the EoS much softer with respect to the pure nucleonic case. This softening is essentially due to a decrease of the kinetic energy because the hyperons can be accommodated in lower momentum states. The softening of the EoS casused by the presence of hyperons has important consequences on many macroscopic properties of the star.

The main consequence of the presence of hyperons in the interior of a neutron star is a substantial reduction of the maximum stellar mass (ΔM_{max} ~ 0.5-0.8 $M_{\odot}$) and the corresponding increase of the central density. In addition, hyperon stars are more compact (i.e., they have a smaller radius) with respect to pure nucleonic stars. This seems to be an inevitable feature of any approach taking into account the presence of hyperons, caused simply by the availability of additional degrees of freedom of the matter at high density, as it is illustrated on the right panels of

Fig. 11. The figure shows the mass-radius and mass-central density relations for different EoS with and without hyperonic degrees of freedom obtained within the BHF approximation (see Ref. [110] for details). Curves labelled APR, V18+GLMM and V18+UIX correspond to pure nucleonic EoS´s. Note that in this case the resulting maximum masses are relatively large, ranging from about 1.8 to 2.4 solar masses. Note also that the presence of hyperons induces a strong reduction of the variation of the result with the nucleonic component of the EoS. The maximum masses obtained with the three EoS lie within a range of 0.15 $M_\odot$, compared to a range of 0.5 $M_\odot$ in the case without hyperons. This clearly emphasizes the important and well-known role of the hyperons as equalizing the effects of different nucleonic interactions: a stiffer nucleonic EoS causes an earlier onset and larger cocentration of hyperons and therefore a stronger softening of the total EoS. The resulting maximum mass is surprisingly quite insensitive to the purely nucleonic EoS and even to the details of the YN and YY interactions. There remain, however, characteristic differences between the mass-radius relations that would eventually allow one to determine the EoS from a combined M,R measurement, which is much awaited since a long time.

It is importat to notice that a realiable microscopic EoS of high-density baryonic matter based on realistic NN, YN and YY forces leads to low masses of neutron stars, even below the current observational limit of 1.44 $M_\odot$. This feature is largely independent of the nucleonic part of the EoS due to a strong compensation mechanism caused by the appearance of hyperons. Clearly, one should try to trace the origin of this problem back to the underlying YN and YY two body interactions or to the possible repulsive three-body forces involving one or more hyperons. Presently this is a subject of very active research in this field. Therefore, the use of microscopic EoS's of hyperonic matter in the context of neutron star physics is of fundamental importance for our understanding of strong interactions involving hyperons, and to learn how these interactions behave in dense many-body systems.

V- SUMMARY

The purpose of this lecture has been to present several topics of hypernuclear physics. After an introduction and an historical overview of the field, we have discussed in the first part of the lecture different production mechanism of single-Λ and double-Λ hypernuclei, as well as several aspects of γ-ray hypernuclear spectroscopy and weak decay modes of hypernuclei. During the second part of the lecture we have presented several approaches to build the hyperon-nucleon. In particular we have discussed models for the hyperon-nucleon interaction based on meson-exchange theory, chiral effective field theory and the recent $V_{low\,k}$ approach. Finally, in the last part of the lecture we have examined the role of hyperons on the Equation of State and and structure properties of neutron stars.

Acknowledgements

I would like to thank the organizers of the school F. Azaiez, L. Berthier, G. Chanfray, T. Hennino, D. Lacroix, D. Lhuillier, J. Margueron, M.-G. Porquet, O. Sorlin and J.-M. Sparenberg for inviting me to participate.

REFERENCES

[1] M. Danysz and J. Pniewsli, Phil. Mag. 44, 348 (1953).

[2] M. Juric et al., Nucl. Phys. B 52, 1 (1973).

[3] D. H. Davis, Proc. Of the LAMPF Workshop on (π,K) Physics, AIP Conf. Proc. 224, ed. by B. F. Gibson, W. R. Gibbs and M. B. Johnson, p. 38 (AIP, New York, 1991).

[4] M. Danysz et al., Phys. Rev. Lett, 11, 29 (1963).

[5] D.J. Prowse, Phys. Rev. Lett. 17, 782 (1966); M. Danysz et al., Nucl. Phys. 49, 121 (1963) reanalized in R. H. Dalitz, Proc. Roy. Soc. London A 426, 1 (1989); S. Aoki et al., Prog. Theor. Phys. 85, 1287 (1991); G. B. Franklin, Nucl. Phys. A 585, 83c (1995).

[6] Proceedings Summer Study Meeting on Nuclear and Hypernuclear Physics with Kaon beams, BNL report 18335, edited by H. Palevsky (1973).

[7] W. Brückner et al., Phys. Lett. B 55, 107 (1975); Phys. Lett. B 62, 481 (1976).

[8] R. Bertini et al., Phys. Lett. B 83, 306 (1979); Nucl. Phys. A 360, 315 (1981); Nucl. Phys. A 368, 365 (1981).

[9] R. E. Chrien et al., Phys. Lett. B 89, 31 (1979); B. Povh, Nucl. Phys. A 335, 233 (1980); M. May et al., Phys. Rev. Lett. 47, 1106 (1981).

[10] E. V. Hungerford, Prog. Theor. Phys. Suppl. 117, 135 (1994).

[11] C. Greiner et al., Phys. Rev. D 38, 2797 (1988).

[12] C. B. Dover and A. Gal, Ann. Phys. (N.Y.) 146, 309 (1983).

[13] C. B. Dover et al., Phys. Rev. C 44, 1905 (1991).

[14] R. Engelmann et al., Phys. Lett. 21, 587 (1966).

[15] G. Alexander et al., Phys. Rev. 173, 1452 (1968).

[16] B. Sechi-Zorn et al., Phys. Rev. 175, 1735 (1968).

[17] J. A. Kadyk et. Al., Nucl. Phys. B 27, 13 (1971).

[18] J. Eisele et al., Phys. Lett. B 37, 204 (1971).

[19] K. Migayawa and W. Glöckle, Phys. Rev. C 48, 2576 (1993).

[20] K. Migayawa, H. Kamada, W. Glöcke and V. Stoks, Phys. Rev. C 51, 2905 (1995).

[21] B. F. Gibson and D. R. Lehman, Phys. Rev. C 37, 679 (1988).

[22] A. Bouyssy and J. Hüfner, Phys. Lett. 64B, 276 (1976); A. Bouyssy, Phys. Lett. 84B, 41 (1979).

[23] C. B. Dover, L. Ludeking and G. E. Walker, Phys. Rev. C 22, 2073 (1980).

[24] T. Motoba, H. Bando, T. Fukuda and J. Zofka, Phys. Rev. C 38, 1322 (1988).

[25] D. J. Millener, C. B. Dover and A. Gal, Phys. Rev. C 38, 2700 (1988).

[26] Y. Yamamoto, H. Bando and J. Zofka, Prog. Theor. Phys. 80, 757 (1988).

[27] F. Fernández, T. López-Arias and C. Prieto, Z. Phys. A 334, 349 (1989).

[28] D. E. Lanskoy and Y. Yamamoto, Phys. Rev. C 55, 2330 (1997).

[29] I. Vidaña, A. Polls, A. Ramos and H.-J. Schulze, Phys. Rev. C 64, 044301 (2001).

[30] R. Brockmann and W. Weise, Nucl. Phys. A 355, 365 (1981).

[31] M. Chiapparini, A. O. Gattone and B. K. Jennings, Nucl. Phys. A 529, 589 (1991).

[32] J. Mares and J. Zofka, Z. Phys. A 33, 209 (1989).

[33] N. K. Glendenning, D. Von-Eiff, M. Haft, H. Lenske and M. K. Weigel, Phys. Rev. C 48, 889 (1993).

[34] J. Mares and B. K. Jennings, Phys. Rev. C 49, 2472 (1994).

[35] Y. Sugahara and H. Toki, Prog. Theor. Phys. 92, 803 (1994).

[36] R. J. Lombard, S. Marcos and J. Mares, Phys. Rev. C 51, 1784 (1995).

[37] Z. Ma, J. Speth, S. Krewald, B. Chen and A. Reuber, Nucl. Phys. A 608, 305 (1996).

[38] F. Ineichenm D. Von-Eiff and M. K. Weigel, J. Phys. G 22, 1421 (1996).

[39] K. Tsushima, K. Saito and A. W. Thomas, Phys. Lett. B 411, 9 (1997); K. Tsushima, K. Saito, J. Haidenbauer and A. W. Thomas, Nucl. Phys. A 630, 691 (1998).

[40] Y. Yamamoto and H. Bando, Prog. Theor. Phys. Suppl. 81, 9 (1985).

[41] Y. Yamamoto and H. Bando, Prog. Theor. Phys. 83, 254 (1990).

[42] Y. Yamamoto, A. Reuber, H. Himeno, S, Nagata and T. Motoba, Czec. Jour. Phys. 42, 1249 (1992).

[43] Y. Yamamoto, A. Reuber, H. Himeno, S, Nagata and T. Motoba, Prog. Theor. Phys. Suppl. 117, 361 (1994).

[44] D. Halderson, Phys. Rev. C 48, 581 (1993).

[45] J. Hao, T. T. S. Kuo, A. Reuber, K. Holinde, J. Speth and D. J. Millener, Phys. Rev. Lett 71, 1498 (1993).

[46] M. Hjorth-Jensen, A. Polls, A. Ramos and H. Müther, Nucl. Phys. A 605, 458 (1996).

[47] I. Vidaña, A. Polls, A. Ramos and M. Hjorth-Jensen, Nucl. Phys. A 644, 201 (1998).

[48] N. K. Glendenning, Astrophys. J. 293, 470 (1985).

[49] S. Balberg and A. Gal, Nucl. Phys. A 625, 435 (1997).

[50] S. Pal, M. Hanauske, I. Zakout, H. Stöker and W. Greiner, Phys. Rev. C 60, 015802 (1999).

[51] R. Knorren, M. Prakash and P. J. Ellis, Phys. Rev. C 52, 3470 (1995).

[52] J. Schaffner, C. B. Dover, A. Gal, D. J. Millener, C. Greiner and H. Stöker, Ann. Phys. (N.Y.) 235, 35 (1994).

[53] H. Huber, F. Weber, M. K. Weigel and C. Schaab, Int. J. Mod. Phy. E 7, 301 (1998).

[54] M. Baldo, G. F. Burgio and H.-J. Schulze, Phys. Rev. C 61, 055801 (2000).

[55] I. Vidaña, A. Polls, A. Ramos, L. Engvik and M. Hjorth-Jensen, Phys. Rev. C 62, 035801 (2000).

[56] N. K. Glendenning, *"Compact Stars: Nuclear Physics, Particle Physics and General Relativity"*, Springer-Verlarg, New York, 1997.

[57] M. Prakash, I. Bombaci, M. Prakash, P.J. Ellis, J. M. Lattimer and R. Knorren, Phys. Rep. 280, 1 (1997).

[58] S. L. Shapiro and S. A. Teukolsky, *"Black holes, White dwarfs and Neutron stars"*, John Willey & Sons, New York, 1983.

[59] A. B. Migdal, *"Theory of Fermi Systems and Applications to Atomic Nuclei"*, Wiley Interscience, New York, 1967.

[60] D. Gogny, Nucl. Phys. A 237, 399 (1975).

[61] T. H. R. Skyrme, Phylos. Mag. 1, 1043 (1956); Nucl. Phys. A 9, 615 (1959).

[62] D. Vautherin and D. M. Brink, Phys. Rev. C 5, 626 (1972).

[63] J. W. Negele and D. Vautherin, Phys. Rev. C 5, 1472 (1972).

[64] S. Balberg, I. Lichtenstadt and G. B. Cook, Ap. J. Suppl. 121, 515 (1999).

[65] B. D. Serot and J. D. Walecka, Adv. Nucl. Phys. 16, 1 (1986).

[66] B. D. Serot and J. D. Walecka, Int. J. Mod. Phys. E 6, 515 (1997).

[67] N. K. Glendenning, Phys. Lett. B 114, 392 (1982).

[68] N. K. Glendenning, Z. Phys. A 326, 57 (1987).

[69] M. Agnello et al., Phys. Lett. B 622, 35 (2005).

[70] T. Hasegawa et al., Phys. Rev. C 53, 1210 (1996).

[71] V. Rodrigues, *"Spectroscopic study of Λ-hypernuclei beyond the p-shell region: The HKS eperiment at JLAB"*, Ph. D Thesis, University of Houston, Houston, Texas (2006).

[72] E. V. Hungerford, in *"Topics in Strangeness Nuclear Physics"*, Lecture Notes in Physics 274, Springer-Verlag, 2007.

[73] J. LeRose et al., Nucl. Phys. A 804, 116 (2008).

[74] O. Hashimoto and H. Tamura, Prog. Part. Nucl. Phys. 57, 564 (2006).

[75] M. Ukai et al., Phys. Rev. C 77, 054315 (2008).

[76] W. M. Alberico A. De Pace, G. Garbarino and A. Ramos, Phys. Rev. C 61, 044314 (2000).

[77] A Parreño, in *"Topics in Strangeness Nuclear Physics"*, Lecture Notes in Physics 274, Springer-Verlag, 2007.

[78] M. M. Nagels, Th. A. Rijken and J. J. de Swart, Phys. Rev. Lett. 31, 569 (1973).

[79] R. Machleidt, K. Holinde and Ch. Elster, Phys. Rep. 149, 1 (1987).

[80] U. van Kolck, Prog. Part. Nucl. Phys. 43, 337 (1999).

[81] S. Weinberg, Phys. Rev. Lett. 18, 188 (1967).

[82] G. E. Brown, in *"Mesons in Nuclei"* (M. Rho and D. H. Wilkinson, eds.), Vol I, p. 330, North-Holland, Amsterdam (1979).

[83] B. Holzenkamp, K. Holinde and J. Speth, Nucl. Phys. A 500, 485 (1989).

[84] J. Haidenbauer and U. G. Meiβner, Phys. Rev. C 72, 044005 (2005).

[85] P. M. M. Maessen, Th. A. Rijken and J. J. de Swart, Phys. Rev. C 40, 2226 (1989).

[86] Th. A. Rijken, V. G. J. Stoks and Y. Yamamoto, Phys. Rev. C 59, 21 (1999).

[87] V. G. J. Stoks and Th. A. Rijken, Phys. Rev. C 59, 3009 (1999).

[88] Th. A. Rijken and Y. Yamamoto, Phys. Rev. C 73, 044008 (2006).

[89] M. M. Nagels, Th. A. Rijken and J. J. de Swart, Phys. Rev. D 17, 768 (1978).

[90] S. Weinberg, Phys. Lett. B 251, 288 (1991); Nucl. Phys. B 363, 3 (1991).

[91] P. F. Bedaque and U. van Kolck, Annu. Rev. Nucl. Part. Sci. 52, 339 (2002).

[92] D. Kaplan, *Lectures delivered at the 17th National Nuclear Physics Summer School 2005*, Berkeley, CA, June 6-17, 2005; nucl-th/0510023.

[93] E. Epelbaum, Prog. Nucl. Part. Phys. 57, 654 (2006).

[94] D. R. Entem and R. Machleidt, Phys. Rev. C 68, 041001 (2003).

[95] E. Epelbaum, W. Glöcke and U.-G. Meiβner, Nucl. Phys. A 747, 362 (2005).

[96] H. Polinder, J. Haidenbauer and U.-G. Meiβner, Nucl. Phys. A 779, 244 (2006).

[97] B.-J. Schaefer, M. Wagner, J. Wambach, T. T. S. Kuo and G. E. Brown, Phys. Rev. C 73, 011001 (2006).

[98] O. Elgaroy, L. Engvik, M. Hjorth-Jensen and E. Osnes, Phys. Rev. Lett. 77, 1421 (1996).

[99] N. K. Glendenning, Phys. Rev. D 46, 1274 (1992).

[100] H. Heiselberg, C. J. Pethick and E. F. Staubo, Phys. Rev. Lett. 70, 1355 (1993); Nucl. Phys. A 566, 577c (1994).

[101] D. B. Kaplan and A. E. Nelson, Phys. Lett. B 291, 57 (1986).

[102] Y. Akaishi and T. Yamazaki, Prog. Nucl Phys. 39, 565 (1997).

[103] A. Akmal, V. R. Pandharipande, Phys. Rev. C 56, 2261 (1997).

[104] R. C. Tolman, Phys. Rev. 55, 364 (1939).

[105] J. R. Oppenheimer and G. M. Volkoff, Phys. Rev. C 55, 374 (1939).

[106] J. B. Hartle, Ap. J. 150, 1005 (1967).

[107] V. A. Ambartsumyan and G. S. Saakyan, Sov. Astron. 4, 187 (1960).

[108] I. Vidaña, I. Bombaci, A. Polls, A. Ramos, Astron. Astrophys. 399, 687 (2003).

[109] N. K. Glendenning and S. Moszkowski, Phys. Rev. Lett. 67, 2414 (1991).

[110] H.-J. Schulze, A. Polls, A. Ramos and I. Vidaña, Phys. Rev. C 73, 058801 (2006).